Remote optical fiber sensor with Raman amplification

Thiago V. N. Coelho*[a,b], A.Guerreiro[a], Pedro A. S. Jorge[a], M. J. Pontes[b]
[a]INESC Porto – Dept. of Physics, 687 Rua do Campo Alegre, Porto, Portugal 4150-179;
[b]Dept. of Electrical Engineering , UFES, 514 Av. Fernando Ferrari, Vitória, Brazil 29.060-970

ABSTRACT

In this work, we analyze a remote optical sensor system composed of two Fiber Bragg Gratings (FBGs) and one Long Period Grading (LPG) capable of simultaneously sensing the temperature and the refractive index, separated by 50 km from the optical source and the interrogation unit. Since the active components of the system and the sensor head are separated over such a large distance, it is necessary to consider Raman amplification o strengthen the optical signal. We present both experimental measurements and the results of numerical simulations, which describe the signal evolution and predict the measurement results for a remote sensor based on a LPG. The simulation codes are also used to study a hybrid sensor composed of two FBGs with a LPG. We show that the power ratio between the two central wavelengths of the FBG has a linear relation with the change of refractive index of the sensored medium.

Keywords: Optical Sensor, Fiber Bragg Gratings, Long Period Gratings, Raman Amplification

1. INTRODUCTION

Fiber optical sensors based on Fiber Bragg Gratings (FBGs) and Long Period Gratings (LPGs) are optical fiber devices widely used for monitoring several environmental parameters (including temperature, pressure, refractive index, etc.), which can be used in places with high electromagnetic radiation, in situations with difficult access and for monitoring structural health, thanks to their small size and facility to be integrated into the optical network systems. The progress in optical telecommunications has provided a better cost-effective relation of optical devices and allows the use of communications network infrastructure for remote sensing. For these sensor schemes to monitor large areas it is necessary to consider optical amplification, which can affect the quality of the optical signal and decrease the sensitivity of the monitoring systems.

In recent years, the advancement in the production of optical fibers has enabled optical communications systems to operate over distances of hundreds of kilometers. However, optical fiber sensors have yet to accomplish a similar realization. This limitation arises from different factors, including the use of large bandwidth and incoherent sources, as well as, the interrogation techniques and of the low spectral efficiency modulated formats presently used. But most of all, to develop measurement in remote sites it is necessary to incorporate optical amplification in the sensor systems to overcome link attenuation and propagation losses.

The most mature and available technologies to amplify the optical signal are Erbium Doped Fiber Amplifiers (EDFAs) and Raman Amplification. Unlike EDFA, which needs a special fiber (an erbium doped fiber) to amplify the signal and has a limited amplification bandwidth, the Raman amplifiers use standard fibers and have a gain bandwidth which can be modified by adequately choosing the number, power and central wavelength of the pumps. This promotes Raman Amplification as the best amplification technology for remote sensing.

In this paper, we present a numerical model that describes the propagation and interactions of the pumps and the sensor signal along the fiber. This model is validated by the comparison of the experimental and simulation results applied on the LPG sensor. This model was also used to simulate a Hybrid sensor configuration. The first section outlines different sensoring technologies based on gratings and introduces the Hybrid sensor configuration and the general scheme of using Raman amplification for remote sensing . In the section two, we discussed the methodologies used in this work, explaining the modifications made on the simulation model introduced by Coelho et al.[6] for the case of remote sensing. The third section presents the experimental and simulation results and section four presents the conclusion of this work.

International Conference on Applications of Optics and Photonics, edited by Manuel F. M. Costa,
Proc. of SPIE Vol. 8001, 800146 · © 2011 SPIE · CCC code: 0277-786X/11/$18 · doi: 10.1117/12.892187

1.1 Optical Sensors Based on Fiber Gratings

The optical fiber sensors are based on the idea that some environmental parameters can be imprinted on the intrinsic characteristics of light such as intensity, frequency, phase or polarization. This imprint can be due to many sensing principles, including opto-mechanical effects[2] and changes in the refractive index of optical fibers[3]. In comparison with other types of sensors technology, optical fiber sensors and more specifically sensors based on gratings are small in size, have electromagnetic immunity, can be easily embed into structures such as buildings and bridges, resist to corrosion in water, have long expected lifespan and the capacity to be multiplexed[3,4].

Gratings consist of periodic modulations of the refractive index of the optical fiber, usually induced by photosensitivity, which give a specific spectral response to the fiber. Optical sensors based on gratings can be divided into two categories: FBGs and LPGs. In FBGs, for wavelengths λ_{ress} satisfying a phase match condition given by

$$\lambda_{ress} = 2n_{eff}\mathbf{\Lambda}_{FBG}, \tag{1}$$

where n_{eff} is the effective refractive index and $\mathbf{\Lambda}_{FBG}$ is the grating period, there is a strong coupling between the forward and backward modes of light in the core. As a consequence, there is a strong peak in the spectrum of the backward modes for λ_{ress}. This resonance can be affected by environmental conditions, such as temperature or mechanical stress, which can change the values of both n_{eff} and of $\mathbf{\Lambda}_{FBG}$, thus shifting the resonance peak and allowing to sense the environmental parameters.

LPGs are often applied for sensing the environmental refractive index because it is possible to couple light of the forward core mode with one or more forward cladding modes according to the resonance condition:

$$\lambda_{ress}{}^{m} = [neff^{co} - neff^{cl,m}]\ \mathbf{\Lambda}_{LPG} \tag{2}$$

where λ_{ress} is the wavelength resonance, *m* is the order of the cladding mode, $n_{eff}{}^{co}$ and $n_{eff}{}^{cl}$ are respectively the core and the cladding effective refractive index and $\mathbf{\Lambda}_{LPG}$ is the grating period. Notice that, according to expressions (1) and (2), for the same resonance wavelength $\lambda_{ress} = \lambda_{ress}{}^{m}$ we have that $\mathbf{\Lambda}_{FBG} << \mathbf{\Lambda}_{LPG}$, i.e. the typical grating period of LPGs is much longer than of FBGs and therefore more easier to be produced and less costly. Moreover, the resonance condition of LPGs is a direct function of the effective cladding mode and therefore the sensitivity to the environment is enhanced. On the other hand, FBGs have the advantage of working in reflection even though LPGs have higher sensibilities.

In our case, the sensor is responsive to temperature and changes of the environmental refractive index. The sensitivity to temperature is due to thermal-optic effects, which affect the refractive index of the core, and to the thermal expansion of the fiber, which increases the grating period. On the other hand, the FBG is not intrinsically sensitive to changes of the environmental refractive index, and another sensing principle must be used. By removing part of the coating of the fiber, the core modes can couple more strongly with the external medium and the effective refractive index becomes dependent on the refractive index of the external environment.

1.2 Raman Amplification

Raman scattering is a nonlinear effect which results from the interaction between incident photons and the silica molecules in the optical fibers leading to an inelastic scattering of light over different frequencies and resulting in an energy loss. This effect is usually divided into the Spontaneous Raman Scattering and the Stimulated Raman Scattering (SRS).

The Spontaneous Raman Scattering (SRS) can cause either a frequency upshift or downshift. Downshifts occur when the silica molecules are excited by the incident photons with frequency ω_{inc} (see Fig.1-a) into an unstable virtual state which may decay to a vibrational state with energy higher than the initial ground state. Hence, the photons emitted in the decay process have a smaller frequency ω_S, usually called Stokes frequency.

Sometimes the silica molecules are already in a vibrational state due, for instance to thermal excitations (see Fig. 1-b). As these molecules interact with the incident photons, they are initially excited to a virtual state and may then decay to the ground state. In this case, the emitted photons have a higher energy, resulting in an upshifted frequency ω_{AS}, usually called Anti-Stokes frequency.

Figure 1. (a) The Spontaneous Raman Scattering with Stokes frequencies (b) The Spontaneous Raman Scattering with anti-Stokes frequencies.

The signal amplification is based on SRS and can be understood as an energy transfer from one or more pumps produced by high power CW lasers into the signal which conserves the original phase and frequency of the signal.

A numerical model[6,7] was used to describe the signal and pump propagation in the fiber taking into account Raman Amplification effects, the single and double Rayleigh scattering, the amplifying spontaneous emission (ASE) noise, polarization effects and the interaction between signal and pumps, signal-signal and pump-pump. The main equation is [6]:

$$\frac{dP_\nu^\pm}{dz} = \mp\alpha_\nu P_\nu^\pm \pm {}_\nu P_\nu^\mp$$

$$\pm P_\nu^\pm \sum_{\mu>\nu} \frac{C_{R\mu\nu}}{\Gamma}(P_\mu^+ + P_\mu^-)$$

$$\pm 2\hbar\nu B_e \sum_{\mu>\nu} \frac{C_{R\mu\nu}}{\Gamma}\left(P_\mu^+ + P_\mu^-\right)[1+\eta(T)]$$

$$\mp P_\nu^\pm \sum_{\mu<\nu} \frac{\omega_\nu}{\omega_\mu}\frac{C_{R\nu\mu}}{\Gamma}(P_\mu^+ + P_\mu^-)$$

$$\mp P_\nu^\pm \sum_{\mu<\nu} \frac{\omega_\nu}{\omega_\mu}\frac{C_{R\nu\mu}}{\mathcal{e}}[1+\eta(T)]4\hbar\mu B_e \qquad (4)$$

where P_μ, P_ν, α_μ e α_ν are the powers and attenuation coefficients of the frequencies μ and ν respectively, the superscripts + and – indicate the forward and backward propagation in the z axis direction, $C_{R\mu\nu}$ is the Raman gain efficiency between the frequencies μ and ν, Γ is the polarization factor and takes as a value 1 if the polarizations are preserved and two case the polarizations are not maintained, □ν is the Rayleigh scattering coefficient and B_e is noise bandwidth considered.

1.3 The Hybrid LPG/FBG Sensor

In this work a hybrid sensor was used to measure temperature and refractive index simultaneously[5] which combines the strengths of both FBGs and LPGs, The structure of this sensor head was developed by Jesus et al.[5] using one LPG and

two FBGs to measure environmental temperature and refractive index simultaneously. Fig. 2 shows the schematic of the sensor head and setup used by Jesus et al[5].

The LPG used has a sensibility of 95 pm/0.001 RIU and 98 pm/^{0}C in the resonance wavelength of 1545 nm. The FBGs are quiet insensible to refractive index changes and exhibits a sensibility of 10 pm/^{0}C. The optical fiber was immerse on a test liquid for the measurement of the environmental refractive index.

This sensor configuration permits determine the changes in the refractive index by measuring the reflected power ratio between two FBGs resonance wavelength. The power ratio exhibits a linear dependence with the RIU and the dynamic range is a function of FBGs and LPG position, the LPG bandwidth and the gratings sensibilities.

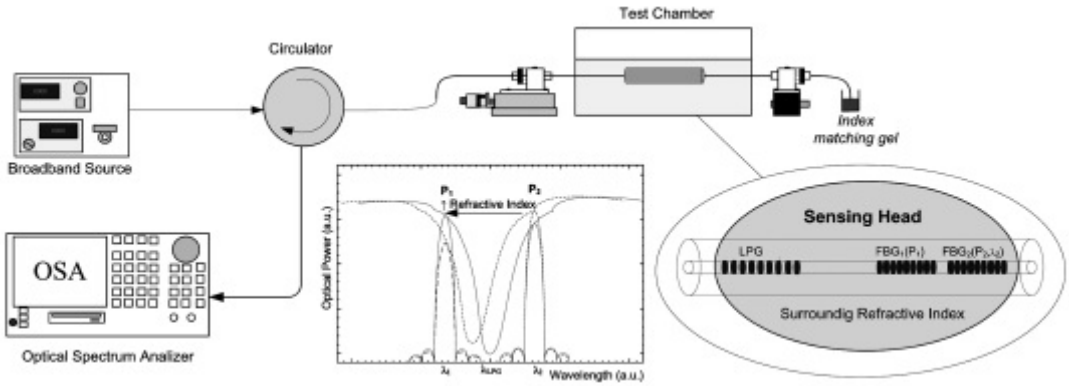

Figure 2. Hybrid sensor head setup.

2. METHODOLOGY

The propagation equations (4) for the source, signal and the pumps was solved using the MatLab® BVP packet and imposing the necessary boundary conditions using known values of the signal in some positions along the fiber. In the simulations, the source signal is propagated along the fiber until it reaches the sensor at the end of the fiber and reflects back the signal to be measured. To validate the model, we consider a LPG sensor and compared the results of the simulation with the experimental measurements obtained using the setup described in Fig. 3.

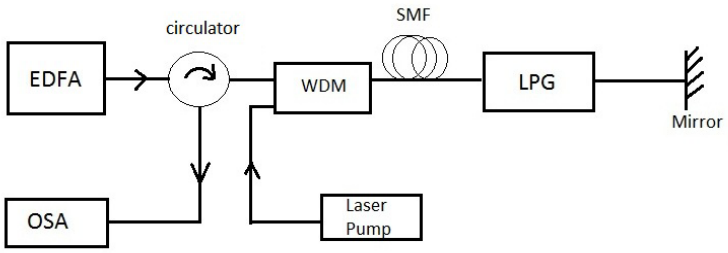

Figure 3. LPG remote sensor setup with Raman amplification applied in the LPG signal

The signal used was a broadband ASE source and the pump laser is a stable coherent high power source with wavelength centered in 1450 nm. The resonance wavelength of the LPG is near 1545 nm, the optical fiber used was the SMF 28 Corning and the mirror has 50% reflectivity in the entire spectral bandwidth of the ASE source. The Fig. 4 shows the spectral source measured at the reflected sensor output.

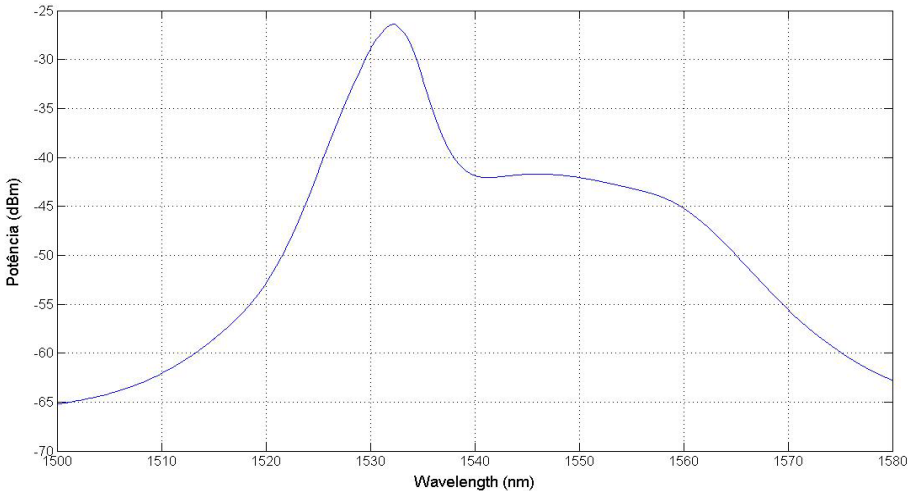

Figure 4. ASE broadband source

The boundary conditions used for the sensor system are similar but not exactly equal to those considered in telecommunications systems. Like in the later, it is considered that there are four light sources injected in the fiber: a forward signal and a forward pump or pumps, which are injected in the beginning of the fiber, and a backward signal and backward pump, which are injected at the end of the fiber, as depicted in Fig. 5. However, unlike the telecommunications systems where the backward signal and pump are usually null, in the case of the sensor the backward signal results from the transmitted forward signal as it is reflected in the sensor head. Since there is a detuning between the forward pump and the reflection wavelength of the sensor head, it is possible to neglect the reflected pump signal and consider the backward pump as null.

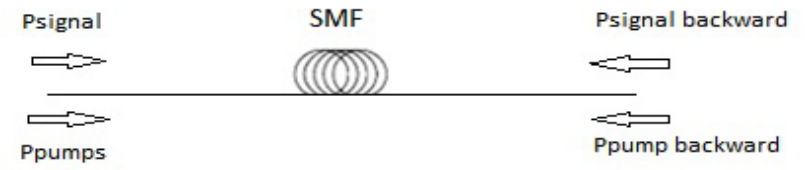

Figure 5. Boundary conditions applied in the numerical solution.

Unfortunately, it is impossible to know *a priori* the backward signal without having computed the transmission of the forward signal and pumps along the fiber. To overcome this difficulty we applied the numerical solution in three steps: i) First we assume that both the backward signal and pump are null and propagate the forward signal and pump along the fiber using values identical to the experimental setup. ii) Then, using the reflection characteristics of the sensor head, we compute the reflected signal. iii) Finally, we repeat the first step but consider that the backward signal is identical to the value obtained in the step ii). This code was used to simulate not only a simple sensor head with just a LPG, which was used to validate the code, but also the hybrid sensor consisting of two FBGs and one LPG for different environmental refractive indexes.

3. RESULTS

In Fig. 6 it is shown the experimental and simulation results for the setup shown in Fig. 2 used to validate the numerical method, where the sensor head consists only of an LPG. The fiber used is a 50 km Corning SMF 28 and the power of the pump laser varies from 400 mW to 1W.

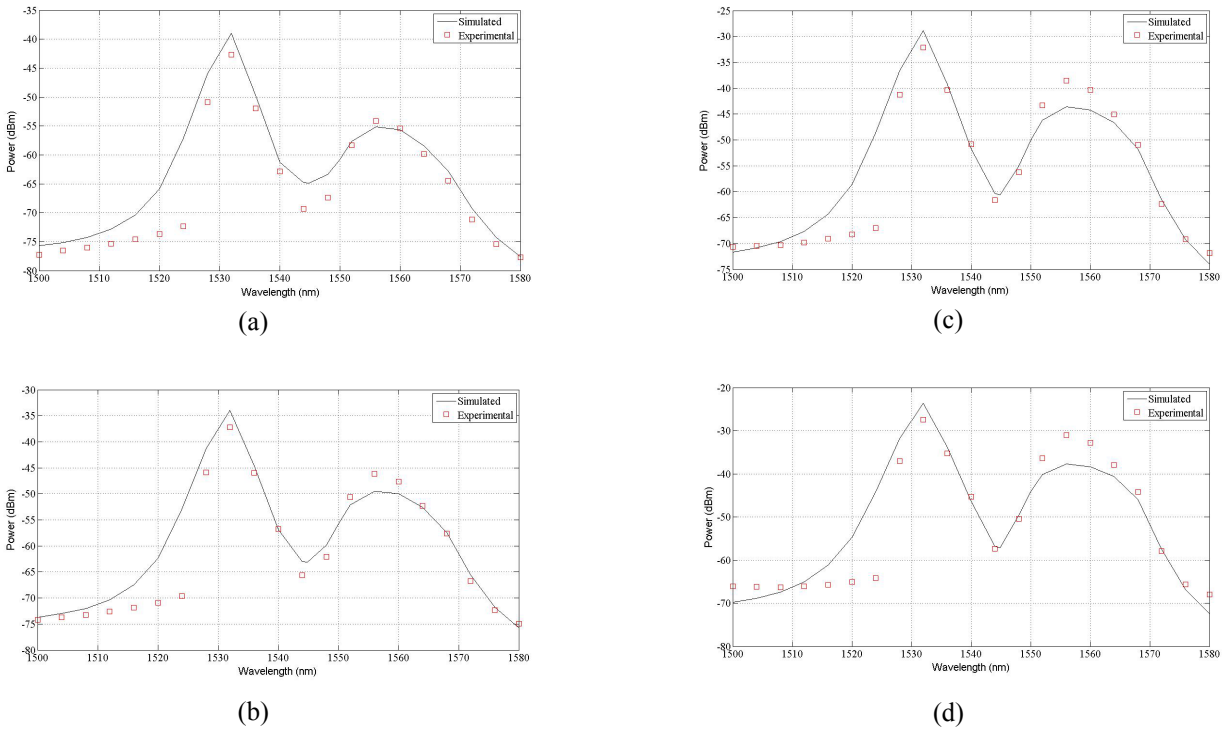

Figure 6 – The experimental and simulation results for the setup in Figure 2 using a laser pump with (2) 400 mW, (b) 600 mW, (c) 800 mW e (d) 1000 mW.

The results shown in Fig. 6 demonstrate that the numerical simulations can effectively reproduce the main features observed in the experiment. The main differences occur for lower wavelengths in the spectrum where the simulations predict a higher power than is measured in the experiment. This can be accounted by the small number of sampling points of the spectrum used in the simulations which results in an underestimation of the transference of power from the low to the high wavelengths.

After validating the numerical method, the same method was applied to the hybrid sensor described in Section 1.3 to study the impact of measure of the index refraction. Fig. 7 shows the relation of the power ratio (parameter R) between the FBGs and the refractive index changes obtained from the simulations. The FBGs are centered around 1535.5 nm and 1546.5 nm, the LPG resonance wavelength is 1542.5 nm with a bandwidth of 15 nm. Two power pumps with 350 mW at 1441.8 and 1444nm were used to provide a better profile of the gain spectrum.

In Fig. 7, we compare the sensitivity of the parameter R with the change of refractive index between a back to back configuration, where the sensor head is connected directly to the interrogation unit (and therefore without amplification) and the remote configuration, where the signal must propagate back along the fiber (and therefore requires amplification). The results show that amplification degrades the sensor sensitivity. An explanation is that in the remote configuration the same optical fiber is used for return channel and for signal amplification. Consequently, the signal is polluted by the ASE noise and the Rayleigh scattering, yielding a degradation of the quality of OSNR ratio. As is shown

in Fig. 8, the power level reflected by the FBG with lowest wavelength has almost the same level as the noise of the optical system. Another problem with this remote configuration is the inefficiency of the amplification since much power of the pumps is used to amplify wavelengths that are rejected by the sensor head and are not represented in the reflected signal.

A simple way to overcome these difficulties is to use two different fibers and separate the channel which connects the source of the signal and the sensor head from the channel of amplification and return of the signal. This reduces both the ASE noise and backward Rayleigh scattering in the return fiber. Other alternative is to use a power splitter and perform a amplification in both fibers.

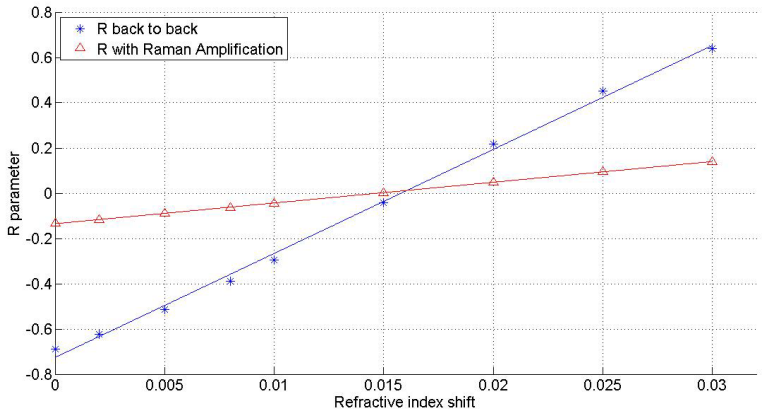

Figure 7 – R parameter vs. Refractive index shift for the back to back and Raman Amplification case

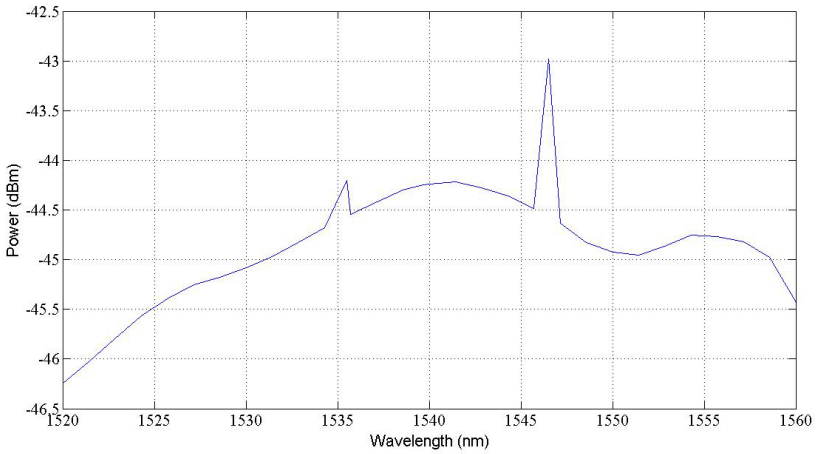

Figure 8 – Optical spectrum in the receiver with an optical noise in the setup used at the figure 7

4. CONCLUSIONS

Sensors based on optical fibers and specially those based on FBGs and LPGs provide low cost and reliable solutions to measure environmental parameters. Many of the existing solutions consider compact devices and are not suited for remote sensing or are focused on distributed sensing[8]. Remote sensing using large spectrum sources (as is the case of

sensors based on FBGs and LPGs) demands optical amplification for the sensor signal to reach the interrogation system with enough quality to be measured with good accuracy.

This work shows the potential of Raman amplification to solve these challenges and presents a numerical model capable of describing the Raman amplification and reproducing the spectrum of a remote LPG sensor with good accuracy around the resonance wavelength.

We also apply this model to study the signal amplification via Raman scattering in an hybrid sensor capable of measuring the environmental refractive index. It was shown that there is a linear relation between the power ratio of the central wavelength of each of the two FBGs however, amplification degrades seriously the sensitivity of the sensor due to the ASE noise and the Rayleigh Scattering. These drawbacks could be solved by replacing the single fiber with two fibers: the first to connect the power source to the sensor head and the second responsible for the transmission of the sensor signal to the interrogation unit. This second fiber can be used either for the Raman amplification or to perform amplification in both fibers via a power splitter.

ACKNOWLEDGMENTS

The first author would like to acknowledge the "CAPES – Coordenação de Aperfeiçoamento de Pessoal de Nível Superior" and "FAPES – Fundação de Amparo a Pesquisa do Espírito Santo" for the support given to the work leading to this article.

REFERENCES

[1] Yin, S., Ruffin, P. B. and Yu, F. T. S., [Fiber Optic Sensors], CRC press, 1-35 (2008).
[2] Mastro, S., El-Sherif, M., "Optomechanical Behavior of Bragg Grating Strain Sensors Under Transverse Load." Proc. IMAC XXIII, (2005).
[3] Chuang, J., Rivera, E., Brown, B. and Flecther, D., "Design and Implementation of an Integrated Fiber Bragg Interrogation System using distributed computing architecture." Proc. Second International Workshop on Structural Health Monitoring of Innovative Civil Engineering Structures; 193-203 (2004).
[4] Kersey, A. D., Davis, A. M., Patrick, H. J., LeBlanc, M., Koo, P. K., Askins, C. G., Putnam, M. A. and Friebele, A. J., "Fiber Bragg Grating Sensors." Journal of Lightwave Technology 15, 1442-1463 (1997).
[5] Jesus, C., Caldas, P., Frazão, O., Santos, J. L., Jorge, P. A. S. and Baptista, J. M, "Simultaneous Measurement of Refractive Index and Temperature Using a Hybrid Fiber Bragg Grating/Long-Period Fiber Grating Configurations." Fiber and Integrated Optics 28, 440-449 (2009).
[6] Coelho, T. V. N., Pontes, M. J., Cani, S. P., "Melhora da Precisão por Conservação de Energia do Modelo Analítico para Amplificadores Raman." Proc. MOMAG, (2010).
[7] Bromage, J., "Raman Amplification for Fiber Communication System." Journal of Lightwave Technology 22, 79-93 (2004).
[8] Xu, Z., Liu, D., Liu, H., Sun, Q., Sun, Z., Zhang, X. and Wang, W., "Design of Distributed Raman Temperature Sensing System Based on Single-mode Optical Fiber." Front. Optoelectron. 2, 215-218 (2009).